

# Replacement Of Mercury With Gallium Alloy In Dental Fills

Dr. Haydar H. J. Jamal Al-Deen\* , Sura Ali Shahee \*\*

**Abstract**— The purpose of this research is to study The replacement of mercury with gallium in dental fills and study of mechanical properties (compression strength, creep, dimensional change, and hardness) and corrosion resistance of dental fills through the use of three types of gallium alloys, which is (Ga- In, Ga- Sn, Ga- In -Sn) and mixed with standard alloy powder (Ardent) and formation of gallium fills. The specimens prepared and tested according to ADA specification No. 1 and kept at  $37\pm 1$  C°. The new alloy has been casted composed of (Ag, Cu, Sn, Zn) for the purpose of improving the properties and especially the dimensional change property where using of liquid (Ga - Sn) because has the best result of the change in dimensions compared with other liquids. All mechanical properties of dental fills were satisfactory as compared to dental amalgam except dimensional change property which was much higher than the allowable limit, The corrosion potential shifting to positive direction, corrosion rate less than amalgam, and the passivation state seem in gallium alloy and did not appear in the amalgam.

**Index Terms**— dental fills; gallium; gallium alloy; replacement of mercury.

## 1 INTRODUCTION

Dental amalgam is one of the oldest materials used in oral health care [1]. It has been estimated that 75 % of all single tooth restoration are amalgam restoration and that this percentage has remained stable for many years [2].

Dental amalgam fillings are widely used over all the world. Their content has about 40-50% mercury (Hg). Therefore, dental amalgam fillings can lead to various side effects and clinical problems [3].

Mercury Only liquid metal at room temperature. The potential toxicity of mercury is the main concern regarding the use of dental amalgam. The use of dental amalgam as a restorative material has long been a contentious issue because of its elemental mercury component [4]. Inhalation and ingestion of mercury from dental amalgam can occur during placement, polishing, removal of restorations or during chewing. The daily dose of mercury from dental fillings, produced by chewing, would appear to amount to 1-2  $\mu\text{g}$ /adult. The threshold for hazard to health from air/mercury exposure in the general population is 5  $\mu\text{g}/\text{m}^2$  air, while it is 1  $\mu\text{g}/\text{m}^2$  for children and pregnant women [5].

Acute inhalation exposure, at high concentrations, may induce respiratory distress including dyspnea , and might cause damage to cardiovascular systems, with increased blood pressure and heart rate. There may also be negative gastrointestinal effects, with abdominal pain and oral

mucositis, fatigue, fever and tremors and even to death. Chronic exposure may induce symptoms from the central nervous system (CNS) including delusions, memory loss and neurocognitive disorders [6].

Nevertheless in the recent past certain drawbacks such as lack of adhesion to tooth structure, marginal leakage and greatest of all, mercury poisoning were noted. Hence, a need for metallic alternative for amalgam led to the development of gallium alloy [7]. Gallium has the second lowest melting point of all metals after mercury (28.9 8C) and has the ability to react with metals and alloys at room temperature to produce a workable plastic mass that hardens with time. As a result Gallium-based alloys have been introduced to the dental market as mercury- free amalgam substitutes which was suggested by Puttkamer as long ago as 1928 [8,9].

Two types of Gallium containing alloys became available for clinical use, those containing palladium at 9% (Gallium Alloy GF, Tokurike Honten, Japan) or 2% Gallium GFII and palladium-free alloys namely Galloy (Southern Dental Industries, Bayswater, Australia). Many studies have been performed to evaluate and develop gallium restorative alloys [10]. The aim of this work is to investigate the replacement of mercury with gallium in dental fills.

- \*Asst. Professor, Dept. of Metallurgical Engineering, Materials Engineering College, University of Babylon, Babylon, Iraq., PH-+9647804168013. E-mail: [jaberjd@gmail.com](mailto:jaberjd@gmail.com)
- \*\*MSc, Dept. of Metallurgical Engineering, Materials Engineering College, University of Babylon, Babylon, Iraq.

## 2 EXPERIMENTAL PROCEDURE

### - Preparation of liquid alloys for fillings

Liquid alloys which used in this work are (Mercury-Gallium alloy), where mercury was used to prepare the amalgam filling, which have been studied as a basis of comparison with other fillings that used liquid gallium based alloy. Three types of liquid gallium alloy have been prepared which is (Ga-In ,Ga-Sn, Ga-In-Sn), which have different degrees of melting, which is (15.5 Co, 20.5 Co, -19.5 Co), respectively as shown in Table.1.

TABLE 1  
Illustrates The Melting Point and The Chemical Composition of Liquid and Powder Used Alloys.

No.	Code	Composition of liquid used				Melting point(Co)	Powder alloy		
		(wt%)					used(wt%)		
		Ga	In	Sn	Hg		Ag	Sn	Cu
1	M	0	0	0	100	-38.83	44.5	30	25.5
2	GI	78.6	21.4	0	0	15.5	44.5	30	25.5
3	GS	86.5	0	13.5	0	20.5	44.5	30	25.5
4	GIS	68	22	10	0	-19.5	44.5	30	25.5
5	G1	86.5	0	13.5	0	20.5	40	40	20

### - Preparation of powder alloys for fillings

All alloys have been prepared which are (M, GI, GS, GIS) using the standard powder (Ardent) made in Sweden which purchased from the market. In addition, we have prepared a new powder alloy, where the chemical composition of this powder shown in Table 2, New powder alloy was mixed with the liquid alloy (Ga-Sn) to prepared (G1) alloy in order to improve the properties. Where the G1 powder alloy was prepared as the follows: The elements (silver, copper, tin and zinc) are melted using electrical furnace and the operation was done under inert atmosphere using argon gas. The ingot that has been obtained by casting was heat treated at 400Co for 4 hours to obtain uniform distribution of the ingot elements and phases. The prepared cast alloy is subsequently transformed into powder. Finally the powder heat treated for stress relief at 100 oC for three hours under vacuum atmosphere.

TABLE 2  
Illustrates The Chemical Composition Analysis of The Powder Alloy Used For Preparation G1 Fill.

Alloy	Ag wt%	Sn wt%	Cu wt%	Zn wt%
Powder alloy	45.46	26.93	24.76	2.85

### 2.2. Specimens Preparation

The specimens were made by trituration of equal weight of powder alloy and mercury (50:50) by amalgamator type (YDM-Pro) for 20 seconds to gallium fill and 30 second of the dental amalgam; their dimensions were 4mm in diameter and 8mm in height using teflon mould. The specimens were prepared according to the American Dental Association (A.D.A.) specification No.1 for dental amalgam [11].

The specimens have been stored at 37±1 C° in glass chamber prepared for this purpose.

### 2.3. Microstructure Characterization

#### - X-Ray Diffraction Analysis

X-ray diffraction analysis has been performed on specimens of each fill to determine the existing phases. X-ray diffraction device used is ( XRD-6000,SHIMADZO Japan) supplied with single wave length Cu - Kα - 1.54 Å, with nickel filter. (20° - 90°) was the range of the diffraction angle.

#### - Microstructure Observation.

The microstructure of a specimen of each alloy was observed and studied using optical microscope and scanning electron microscope (SEM). Wet grinded using different grades of emery papers (180,400, 600, 800, 1200, 1500, 2000, 2500), then polished with cloth using alumina liquid of 0.25 μm particle size. The specimens etched with the nitric acid in concentrations of 30% by volume [12]. Inverted metallurgical microscope is used at 200x magnification in the microstructure examination of the specimens.

### 2.4.Mechanical Properties

Compressive strength was evaluated according to (A.D.A.) specification No.1 [11] by using universal testing machine type WDW- 200 China. The diameter of the specimens was measured with micrometer before the test. The specimen loading speed was for 0.5 mm/ min. The first measurement was done 1 day after the end of trituration; the second was measured after 7 days. The average value of five specimens of each alloy has been reported. The compressive strength is calculated by using the following equation [13]:-

$$\text{Compressive strength} = \frac{\text{Max.force}}{\text{cross sectional.area}} \quad (1)$$

Creep test accomplished according to A.D.A. specification No. 1 [11] at 37± 1 C°, where allows the maximum of 3%

creep. In order to measure the creep, the prepared specimens were stored in an incubator

maintained at  $37 \pm 1$  °C. The length of the specimen should be measured after two hours and 45 minutes from the end °C. This was done in a continuous manner for 21 hours, after which the specimen length was measured again. The average value of three specimens of each alloy has been reported. Creep percent is calculated by using the following equation [11]:-

$$\text{Creep \%} = \frac{L_o - L}{L_o} \times 100 \quad (2)$$

Where

$L_o$  = original length (mm).

L = final length (mm).

Dimensional change performed according to A.D.A. specification No.1, where the first record was taken immediately after specimen was formed (30 minutes for amalgam and 50 minutes for gallium fills after trituration), The specimens were sit free without any restraint during the test. The length of the specimens was measured after 24h after the end of trituration. The specimens were kept at a constant temperature of  $37 \pm 1$  °C at the incubator. The dimensional change must be within range of  $\pm 20$   $\mu\text{m}/\text{cm}$ . The average value of ten specimens of each alloy has been reported.

Vickers microhardness tested in a digital Microhardness tester (Type TH715, Beijing, Time High Technology Ltd), at a static load of 200 g for 10 seconds, that was performed in different time intervals (1 day and 7 days) after the end of trituration. Vickers hardness value obtained directly from the devise. The average value of five specimens of each alloys has been reported, At least three indentations were made at diagonal distribution across the specimen.

## 2.5 Corrosion Test

Potentiodynamic polarization was used as the technique for evaluating corrosion resistance for amalgam and Gallium restorative alloys tested. Computerized potentiostat (Wenking M Lab, Germany) was used for accomplishing the polarization test. The corrosion resistance of specimens was studied in synthetic saliva solution, the pH solution was 6.7 at  $37$  °C temperature. The specimens were tested after 7 days from the end of trituration.

The corrosion test cell used in this study was made according to ASTM standard (G5-87) [12], which including the reference electrode is Saturated Calomel Electrode (SCE), Auxiliary Electrode (Pt.E.) is platinum electrode, and working electrode (specimen). When the specimen reaches the constant potential, potentiodynamic polarization was started from an initial potential of 250 mV below the open circuit potential and the scan was continued up to 250 mV above the open circuit potential for GI dental, up to 350 mV for GIS dental, up to 550 mV for GS and G1, and up to 650 mV for M dental. The corrosion test was carried out at  $37 \pm 1$  °C to stimulate the human body temperature, Two

of trituration. At three hours after the end of the trituration the specimen subjected to a constant axial pressure of  $10\text{MN}/\text{m}^2$  were applied at constant temperature of  $37 \pm 1$

specimens from each fill type were prepared for this test. Corrosion rate measurement is obtained by using the following equation [14].

$$\text{Corrosion Rate (mpy)} = \frac{0.13 i_{\text{cor}} (E.W.)}{A \cdot \rho} \quad (3)$$

where:

E.W. = equivalent weight (gm/eq.).

A = area ( $\text{cm}^2$ ).

$\rho$  = density ( $\text{gm}/\text{cm}^3$ ).

0.13 = metric and time conversion factor.

$i_{\text{cor}}$  = current density ( $\mu\text{A}/\text{cm}^2$ ).

## 3 RESULT AND DISCUSSION

### 3.1 Microstructure Characterization

-X - Ray Diffraction of dental fillings

All fillings studied in this work have been tested by XRD for phases evaluation and Figures (1-5) show the x-ray diffraction patterns obtained from these alloys. The ( $\gamma_1$  ( $\text{Ag}_2\text{Hg}_3$ ),  $\eta$  ( $\text{Cu}_6\text{Sn}_5$ ) and unreacted  $\gamma$  ( $\text{Ag}_3\text{Sn}$ )) phases were existed in M alloy which appear in Figure (1), Where the predominate phase is  $\gamma_1$  which was the matrix of the microstructure. While the XRD analysis of GI alloy is shown in Figure (2) where can be seen Seven different phases in this alloy ( $\text{CuGa}_2$ ,  $\text{Ag}_{0.72}\text{Ga}_{0.28}$ ,  $\text{In}_4\text{Ag}_9$ ,  $\text{Cu}_6\text{Sn}_5$ ,  $\text{Cu}_{16}\text{In}_9$ ,  $\text{Cu}_9\text{Ga}_4$ ,  $\text{Ag}_3\text{Sn}$ ), The major phase was  $\text{CuGa}_2$  which represent the matrix. Phases which appear in the GS alloy are ( $\text{CuGa}_2$ ,  $\text{Ag}_{0.72}\text{Ga}_{0.28}$ ,  $\text{Cu}_6\text{Sn}_5$ ,  $\text{Cu}_9\text{Ga}_4$ ,  $\text{Ag}_3\text{Sn}$ ) which show in Figure (3), The  $\text{CuGa}_2$  phase also represents the matrix of alloy. Figure (4) indicates the phases of GIS alloy. Nine Phases which appear in this alloy are ( $\text{Ag}_{0.72}\text{Ga}_{0.28}$ ,  $\text{InSn}_4$ ,  $\text{CuGa}_2$ ,  $\text{Cu}_{11}\text{In}_9$ ,  $\text{Cu}_{16}\text{In}_9$ ,  $\text{Cu}_9\text{Ga}_4$ ,  $\text{Ag}_3\text{Sn}$ ,  $\text{Cu}_9\text{Ga}_4$ ,  $\text{Cu}_6\text{Sn}_5$ ), The  $\text{Ag}_{0.72}\text{Ga}_{0.28}$  phase (alloy matrix) because this phase has highest intensity peak. While the XRD analysis of G1 alloy is shown in Figure (5) where can be seen Six different phases in this alloy ( $\text{CuGa}_2$ ,  $\text{Ag}_{0.72}\text{Ga}_{0.28}$ ,  $\text{Sn}$ ,  $\text{Cu}_9\text{Ga}_4$ ,  $\text{Cu}_6\text{Sn}_5$ ,  $\text{Ag}_3\text{Sn}$ ). The  $\text{CuGa}_2$  phase has high intensity of peaks therefore it represents the matrix of the G1 alloy, As we can observe appearance Sn remaining phase. The phases of alloys were determined by comparison with standard XRD cards.

### -Microstructure Observation of dental fillings

The microstructure observation of M alloy illustrates in Figure (6) the microstructure of (M); it consists of light gray regions of amalgam matrix of  $\gamma_1$  phase, dark gray regions of the second major phase of  $\eta$  ( $\text{Cu}_6\text{Sn}_5$ ), gray regions of unreacted  $\gamma$  phase regions and  $\gamma_2$  phase appear as black regions distributed in the microstructure. The microstructure of GI alloy shows in Figure (7) where the light gray regions was the microstructure matrix of  $\text{CuGa}_2$  phase while the white color regions represent rich tin element and can be noted in the dark region the presence of

high amounts of copper as well as silver, tin and small amounts of indium and gallium component, and this indicates the presence of more than one phase in this region. Figure (8) exhibits the microstructure of GS alloy, which consists of light gray regions which is the matrix of Ag<sub>0.72</sub>Ga<sub>0.28</sub> phase, gray regions of (CuGa<sub>2</sub>) phases, dark gray regions contained mixture of phases and white regions represent rich tin element. While Figure (9) indicates the microstructure of GIS alloy, the light gray regions was the microstructure matrix of Ag<sub>0.72</sub>Ga<sub>0.28</sub> phase gray region represent of (CuGa<sub>2</sub>) phases while the dark gray region is contain of mixture of phases, The microstructure observation of G1 alloy demonstrates in Figure (10), where the dark gray regions of Ag<sub>0.72</sub>Ga<sub>0.28</sub> phase, also the light gray region contain this phase and CuGa<sub>2</sub> phase which represent the dominant phase in this alloy, All these nearest value to change the dimensions of the allowable limit was (21.1 μm/cm) of alloy GS, Where the allowable limit for dimensional change According to A.D.A. Specification No. 1 is (± 20 μm/cm) [11], therefor, the dimensional change of alloys are exceed A.D.A. limit.

The results obtained from the mean creep value of three specimens of each alloy are shown in Table (3). According to the ADA specification No. 1, the acceptable creep value in a dental amalgam should be less than 3%. The creep value of alloys was high but lower than ADA limit (3%) where the GI alloy was (1.4%), GIS (1.2%), G1 (1.6%) compared with that of amalgam which was (0.3%). While the value of creep in GS is (3.2%) where it is exceeded the allowable ADA limit.

Vickers hardness of all restorative alloys are reported after one and seven days from the end of trituration. The results in Table (3) demonstrate that gallium alloys have hardness lower than amalgam (M) alloy and have varied from each to other according to the composition of the alloys, And also the presence of (Ag<sub>0.72</sub>Ga<sub>0.28</sub>) phase and different quantity of other phases in each alloy led to this variant.

TABLE 3

The Mean Values of The Compressive Strength, Creep, Dimensional Change and Hardness of All Alloys Used.

Alloys	Mean Compressive strength (MPa)		Mean Creep (%)	Mean Dimensional Change (μm/cm)	Mean Hardness (Kg/mm <sup>2</sup> )	
	1 day	7days			1 day	7 days
	M	119.4	176.2	0.3	+5.2	156.6
GI	153.8	255.2	1.4	+47.9	112.2	143.12
GS	288.7	324	3.2	+21.1	129.6	145.10
GIS	134.6	181.4	1.2	+62.4	84.8	129.90

microstructure of alloys approved by the SEM and XRD analysis.

### 3.2.Mechanical Properties

The compressive strength, dimensional change, creep and hardness of all restorative alloys are shown in Table (3), Where The mean value of Compressive strength reported after (1day -7days) from the end of trituration for all alloys. It can be seen from Table (3), that the compressive strength of gallium alloy has higher value compared with amalgam because the presence of (Ag<sub>0.72</sub>Ga<sub>0.28</sub>) phase in gallium alloys which having high compressive strength (15). From dimensional change results which appear in Table (3), it can be concluded that the amalgam dimensional changes are within the standard allowable limit, while gallium alloys Exceeded allowable limit But the

G1	103.7	202.8	1.6	+30.1	45.7	100.90
----	-------	-------	-----	-------	------	--------

### 3.3.Corrosion Test

The electrochemical corrosion of alloys can be conveniently described by the schematic current-potential curves (The polarization curves) are shown in Figures (11-15). The polarization curve of M alloy is shown in Figure (11), Where the corrosion parameters (E<sub>corr</sub> and I<sub>corr</sub>) of this alloy are -149.5 mV and 1.43μA/cm<sup>2</sup>. In cathodic polarization, the current density decreases with increasing potential until reach value of -149.5mV, which is the corrosion potential E<sub>corr</sub>, with increasing potential, anodic polarization starts. The behavior of anodic polarization was active, where the current density increases with increasing potential giving an indication of M alloy dissolution, after then the barrier film formed on the surface and the dissolution current drops, until reaching the last part of polarization curve and then the barrier film was began breakdown at a potential of 810 mV and a current density of 0.00549 mA. The potentiodynamic curve of GI is presented in Figure (12). It revealed an active to passive transition, and had a critical current density (i<sub>c</sub>) of 0.01065 mA and a passivation potential E<sub>pp</sub> of -266 mV. Above the critical passivation potential corresponding to the maximum in the active region, an passive film grows on the surface until reach to a passive current density i<sub>p</sub> of (0.00912 mA) and potential of (-216 mV) where this passive film covers all the surface and take increase in thickness and at the E<sub>break</sub> value of (-79 mV) which represent transpassive region which then begin of passive layer to breakdown with increasing potential. Figure (13) illustrates cathodic and anodic polarization curves of the GS alloy in synthetic saliva. It exhibited an active to passive transition, which is observed at a critical current density (i<sub>c</sub>) of 0.0186 mA and a passivation potential (E<sub>pp</sub>) of (-246 mV). For alloys that can be passivated, Where the passive films formed on the surface and the dissolution current drops, . Upon the arrival of the potential to the value of (-231 mV) the thickness of passive film is increasing, and when reach to the potential of (-68 mV) which represent E<sub>break</sub> at a



passive current ( $i_p$ ) of 0.00929 mA, the passive film begins breakdown with increasing potential in the transpassive region. Figure (14) indicates the potentiodynamic curve for GIS alloy in synthetic saliva solution. The corrosion potential  $E_{corr}$  was -363.7 mV and a corrosion current  $i_{corr}$  was (2.85  $\mu$ A). The current density increase with increasing potential which mean alloy dissolution after the corrosion potential has passed, after then a marked drop in current densities was observed, which the passive films formed, which could also be a barrier to diffusion at  $i_c$  of 0.0226 mA and a passivation potential  $E_{pp}$  of -246 mV. This effect was observed in the anodic part of the curve. The passive film begins increasing in thickness at potential of (-207mV) and it was breakdown at a potential  $E_{break}$  of -178 mV and a passive current density  $i_p$  of 0.0091 mA. Figure (15) offered the potentiodynamic curve for G1 alloy. Anodic dissolution was observed. The  $i_c$  value was 0.0287 mA and  $E_{pp}$  was -206 mV while  $i_p$  was 0.0075 mA and  $E_{break}$  was -163 mV, similar to the behavior of GI, GS, GIS alloys.

Table (4) shows corrosion potential ( $E_{corr}$ ), corrosion current density ( $i_{corr}$ ) and corrosion rate (C.R.) for tested alloys. Where can be noted that gallium alloys (GI, GS, GIS, G1) have less corrosion resistance than the amalgam (M). The reason for this is due to the presence of the (CuGa<sub>2</sub>, Ag<sub>0.72</sub> Ga<sub>0.28</sub>) phase, which that both phases are corrosion prone which is reported by other researchers [16], and the presence of several types of phases accelerate the corrosion due to galvanic effect.

TABLE 3

Illustrates The Corrosion Potential ( $E_{corr}$ ), Corrosion Current ( $i_{corr}$ ), Corrosion Rate.

Alloy	Mean $E_{corr}$ (mV)	mean $i_{corr}$ ( $\mu$ A/cm <sup>2</sup> )	Corrosion Rate (mpy)
M	-149.5	1.43	7
GI	-375.8	13.75	52.1
GS	-359	15.5	57.2
GIS	-360.7	14.7	56.2
G1	-332.7	6.24	23.69

## 4 CONCLUSION

1. The predominant phase is CuGa<sub>2</sub> in the GI, GS and G1 alloys and Ag<sub>0.72</sub>Ga<sub>0.28</sub> phase in the GIS alloy while the major phase in amalgam is  $\gamma$ 1 phase.
2. Compressive strength of gallium alloy has higher value compared with amalgam.
3. Creep result of GI alloy was (1.4%), GIS (1.2%), G1(1.6%) compared with amalgam were high but did not exceed allowable limit by ADA which is (3%). While the value of creep in GS is (3.2%) where it is exceeded ADA limit.

4. The dimensional change result of all gallium alloys was high, where it is not fall within the standard value according to ADA specification No. 1 which is (20 $\mu$ m / cm) but nearest result of this limit is GS alloy which is (21.1 $\mu$ m / cm).

5. The results indicate that the hardness of all gallium alloys was good but less than amalgam, The G1 alloy has lowest value of hardness.

6. The corrosion rate of gallium alloys was higher than that of amalgam we note the passivation state, which did not appear in the amalgam.

## 5 ACKNOWLEDGMENT

I wish to thank Babylon University/ college of materials engineering/ department of metallurgical engineerin. This work was accomplished at laps of the college.

## 6 REFERENCES

- [1] G. Schmalz and D. Arenholt-Bindslev, "Biocompatibility of Dental Materials" Springer-Verlag Berlin Heidelberg, 2009.
- [2] M. A. Meftah "Mechanical and corrosion improvement of dental amalgam using Zinc Oxide and Titanium Oxide particles". MSc. Thesis, University of Babylon at Iraq, 2014.
- [3] A. Akbal, H.Yilmaz, E. Tutkun and D. Mehmet Kos "Aggravated neuromuscular symptoms of mercury exposure from dental amalgam fillings" Journal of Trace Elements in Medicine and Biology., Vol. 28, pp. 32- 34, 2013.
- [4] H.K. Yip Hong Kong SAR, T. C. Wellington "Dental amalgam and human health" FDI\World Dental Press Vol.53, pp. 464-468,2003.
- [5] J. C. Taggart "Handbook Of Dental Care: Diagnostic, Preventive and Restorative Services" Nova Science Publishers, Inc., 2009.
- [6] T. Syversena and P. Kaur "The toxicology of mercury and its compounds" Journal of Trace Elements in Medicine and Biology, Elsevier GmbH, Vol. 26, pp. 215-226, 2012.
- [7] R. Singh, S. Tandon and M. Rakhee, "Comparative Evaluation Of Clinical Efficacy Of Gallium And Amalgam Alloys In Primar
- [8] F. J. Shainia, F. K. Wahaba, G.P. Flemingb, P. M. Marquisb and A. C. Shortallb "A palladium-free gallium-based alloy: analysis of composition and microstructure" Elsevier Ltd, Vol. 19, pp. 653-661, 2003.
- [9] S. M. Dunne and R. Abraham "A study into the performance of a gallium-based restorative material" British Dental Journal, Vol. 189, No. 6, 2000.
- [10] H. H. Jaber "Study of Gallium Based Restorative Alloy," Journal of Babylon University/Pure and Applied Sciences, No.2, Vol.22, pp. 914-923, 2014.
- [11] A.D.A., "Guide to Dental Materials and Devices, " 7th edition, 1974-1975.
- [12] H. H. Jaber "The effect of admixed Ti on corrosion resistance of high copper dental amalgam, " J. of

Babylon University, Engineering Sciences, Vol. 22, No.2, pp. 413-421, 2014.

- [13] H. H. J. Jamal Al-Deen, A. H. Haleem and M. S. Tuma "Improvement of Dental Amalgam Properties By Increasing Copper Content" International Journal of Scientific & Engineering Research, Vol. 5, pp. 730-737, 2014.
- [14] "Electrochemistry and Corrosion: Overview and Techniques " Application Note CORR-4, 2004, Princeton

Applied Research Electrochemical Instruments Division , 2009.

- [15] Haydar Hassan Jaber "Study of (Ag<sub>0.72</sub> Ga<sub>0.28</sub> and CuGa<sub>2</sub>) Gallium Restorative Phases" The Iraqi Journal for Mechanical and Materials Engineering, No.2, pp. 19-30, (2013).
- [16] H. Hero, T. Okabe, H. Wie " Trace elements in persons with dental amalgam" Journal Of Materials Science, Vol.8, pp. 357-360,1997.

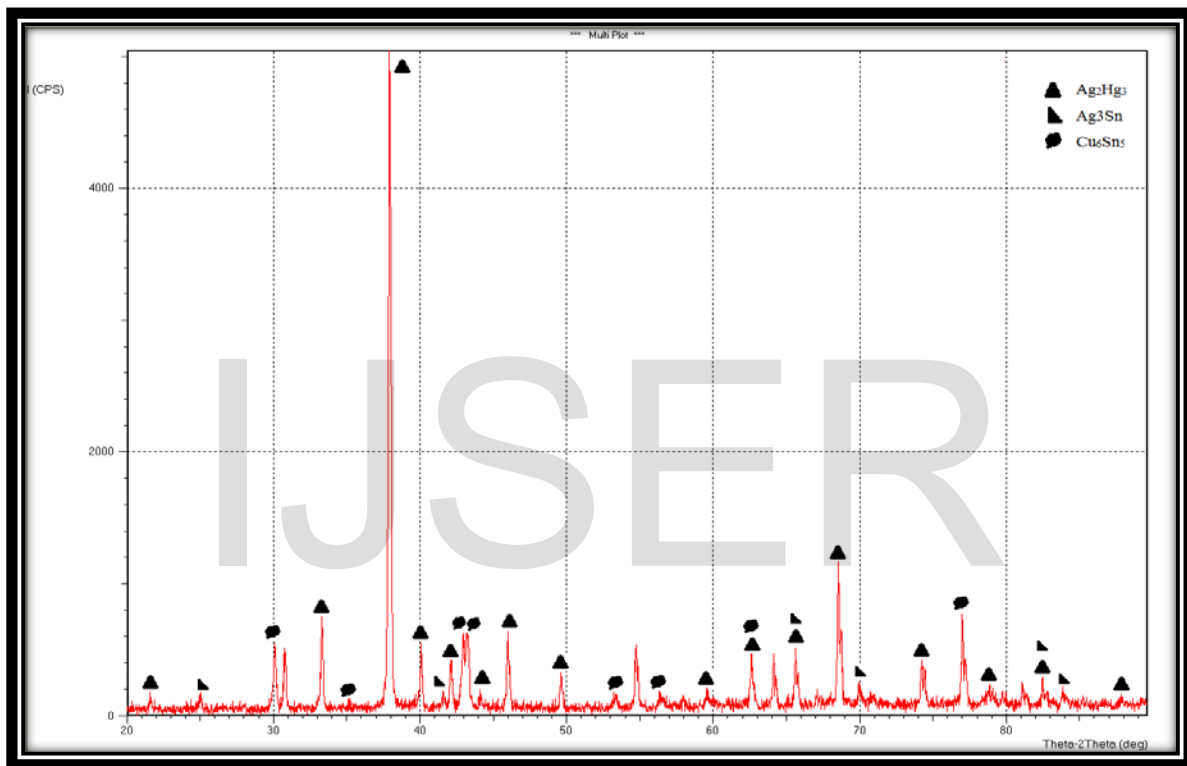


Figure (1) XRD patterns of M alloy.

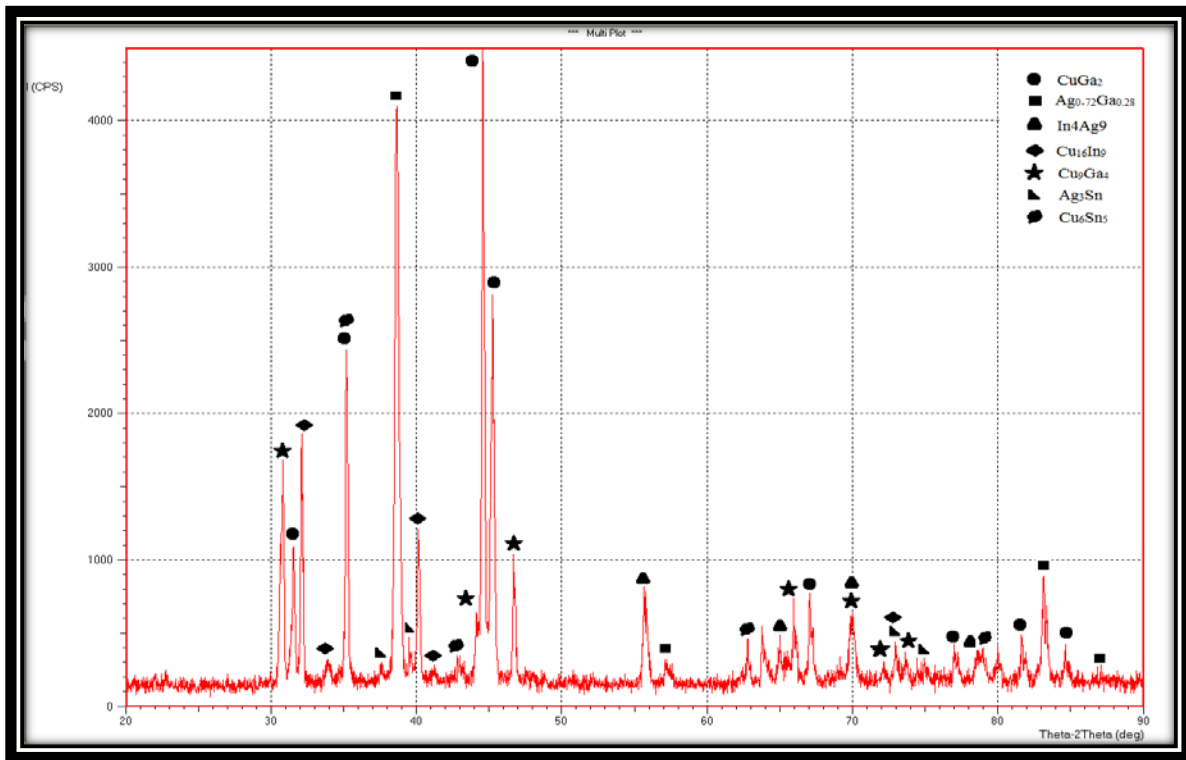


Figure (2) XRD patterns of GI alloy.

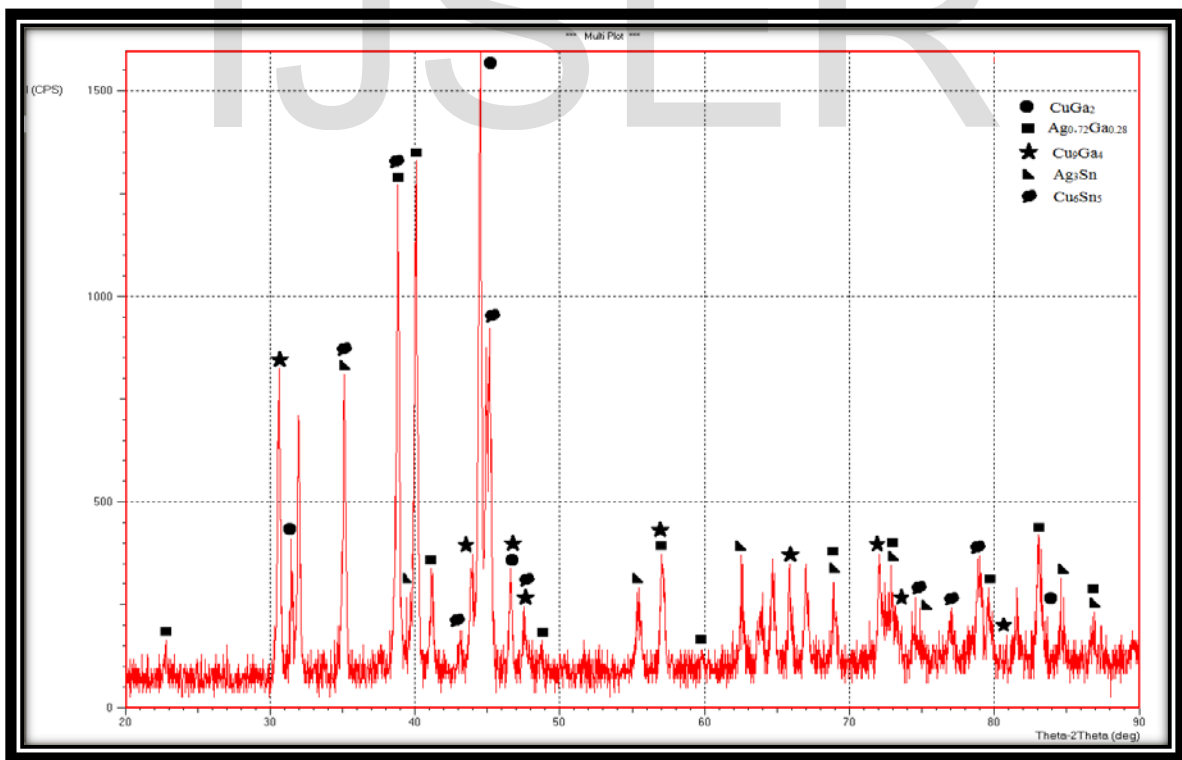


Figure (3) XRD patterns of GS alloy.

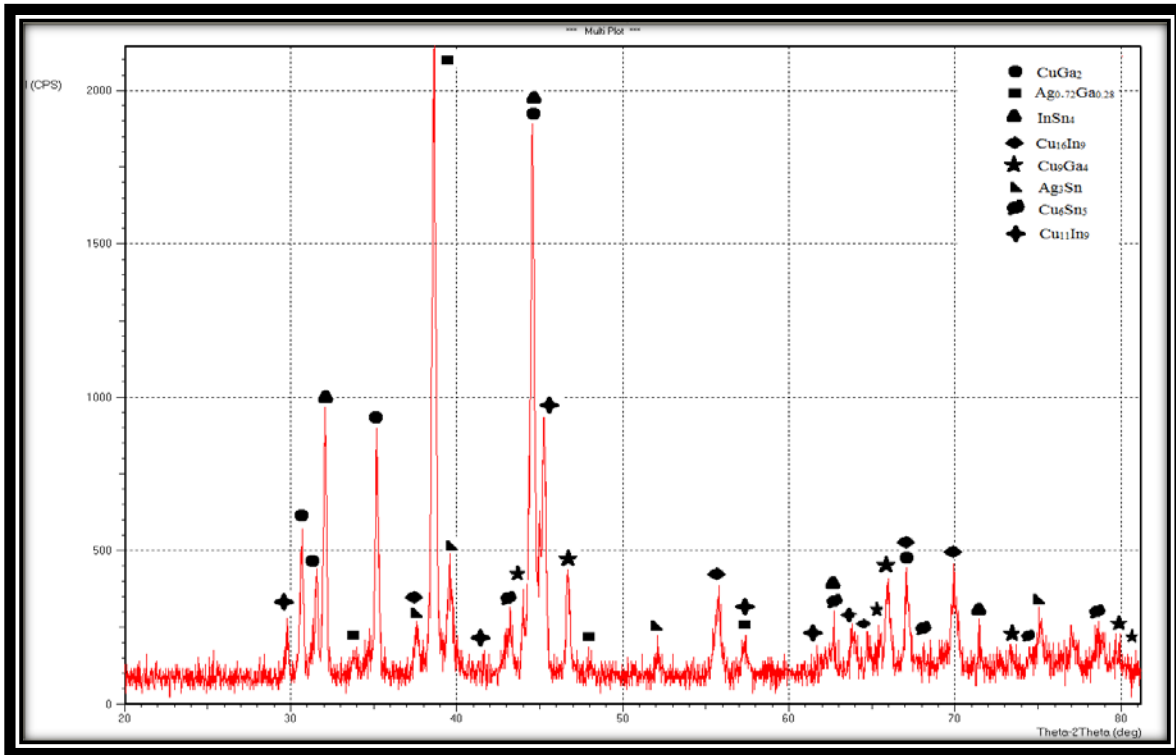


Figure (4) XRD patterns of GIS alloy.

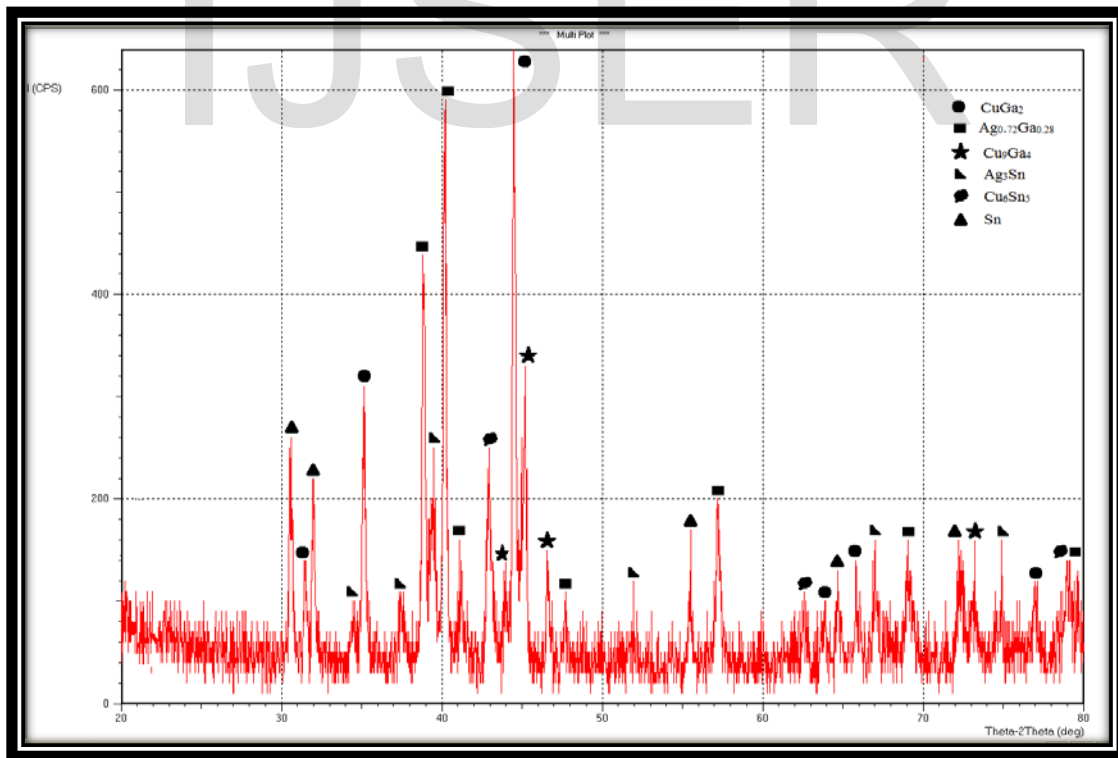


Figure (5) XRD patterns of G1 alloy.



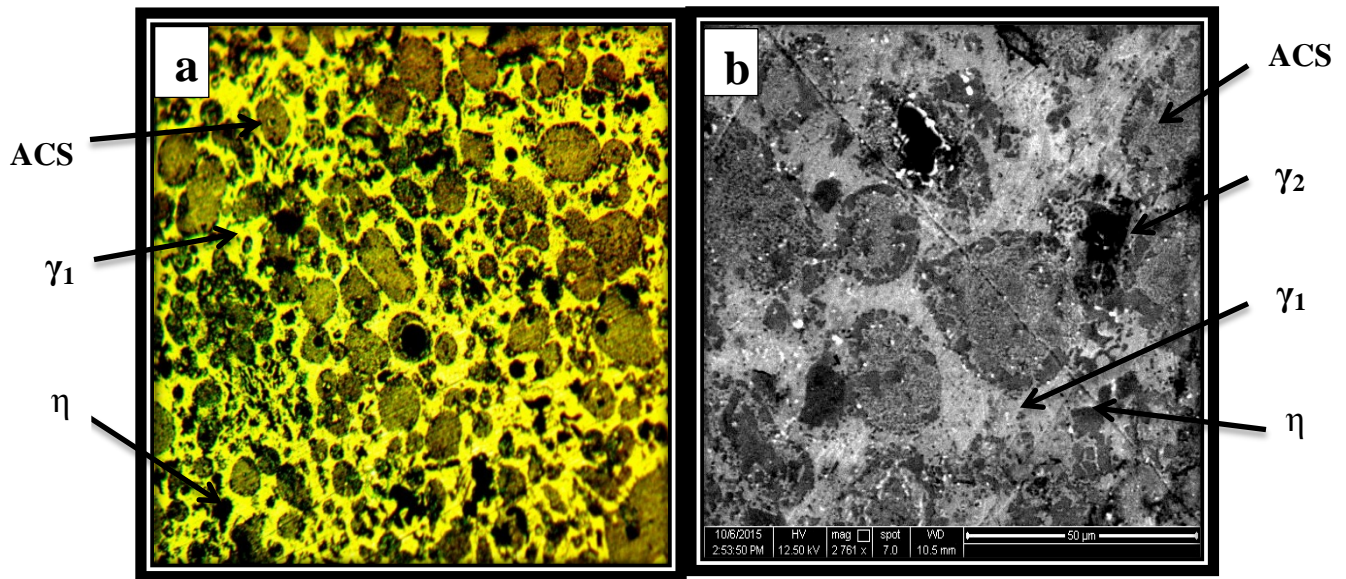


Figure (6) the microstructure observation of amalgam (M) alloy.

a- By Optical Microscope at 400X magnification, b- By SEM where ACS (Ag-Cu-Sn).

IJSER

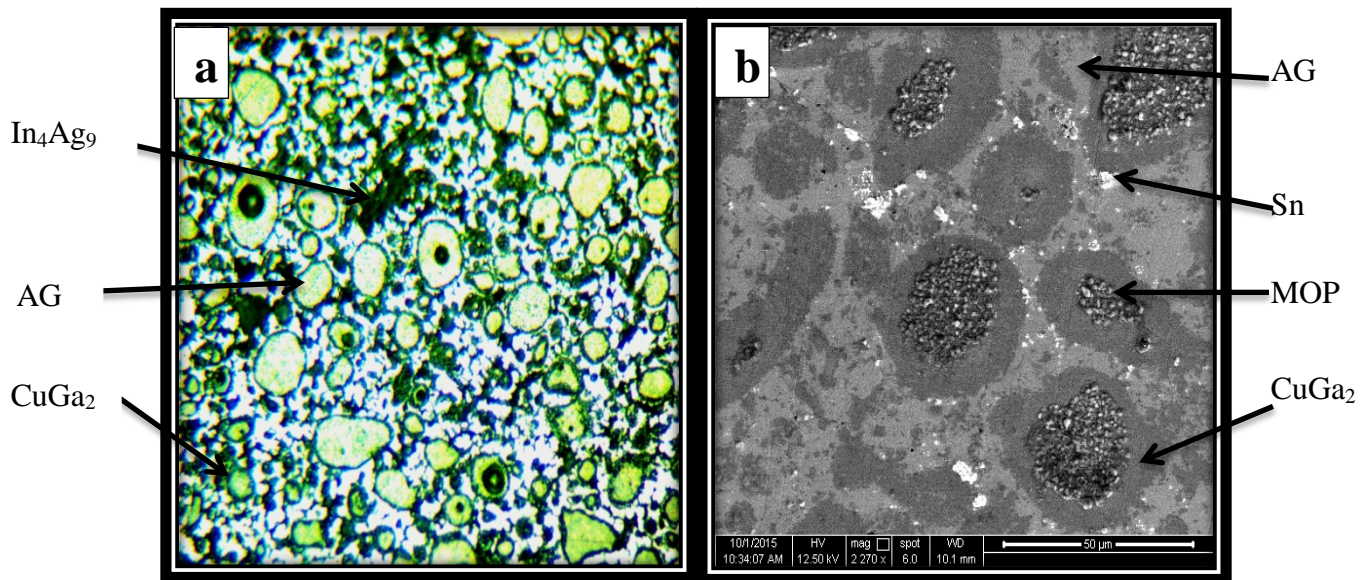


Figure (7) the microstructure observation of GI alloy.

a) By Optical Microscope at 400X magnification, b) By SEM where MOP (mixture of phases), AG( $\text{Ag}_{0.72}\text{Ga}_{0.28}$ ).



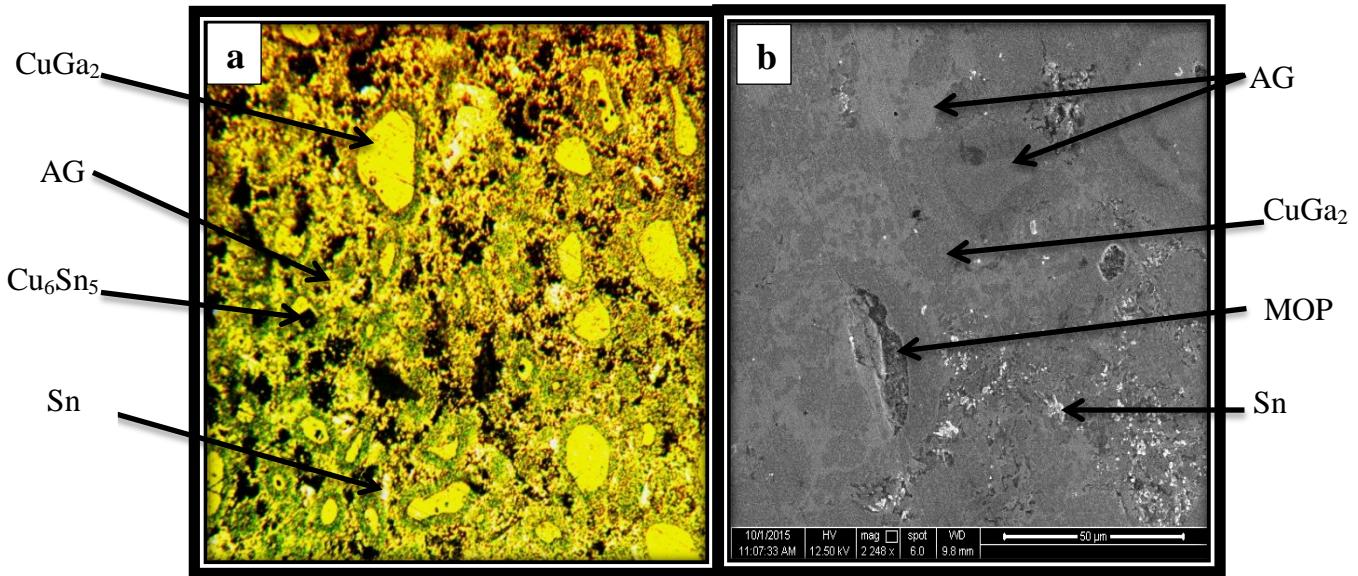


Figure (8) the microstructure observation of GS alloy.  
a) By Optical Microscope at 400X magnification, b) By SEM.

IJSER

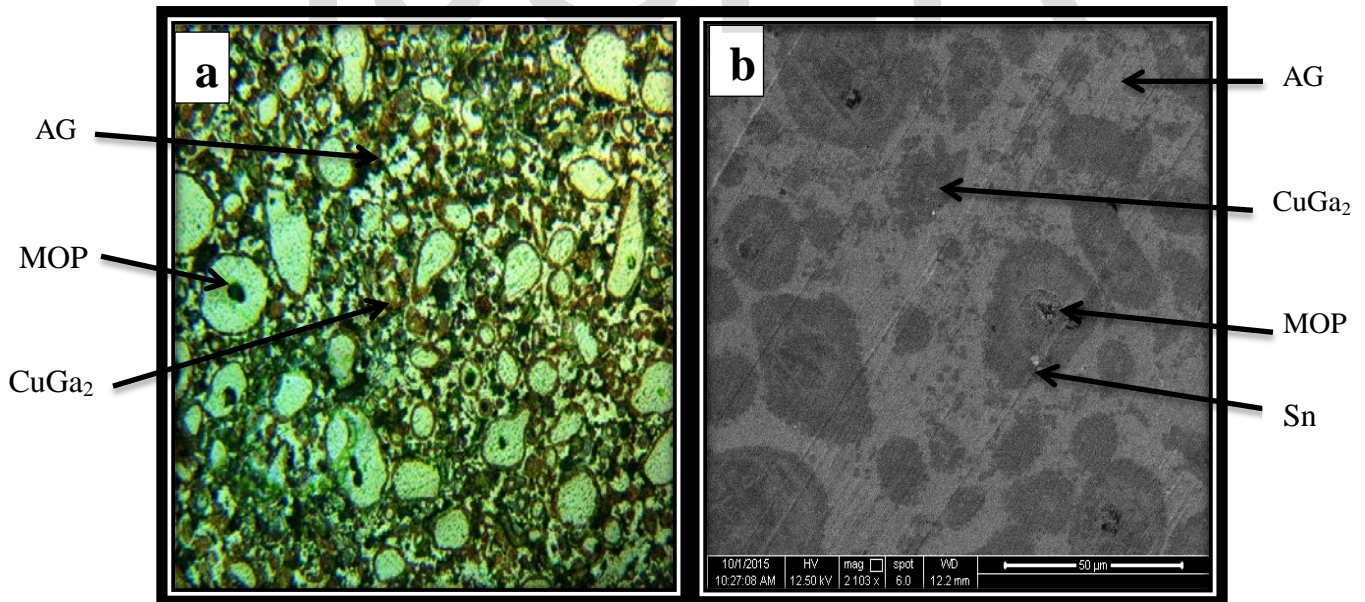


Figure (9) the microstructure observation of GIS alloy.  
a-By Optical Microscope at 400X magnification, b- By SEM.

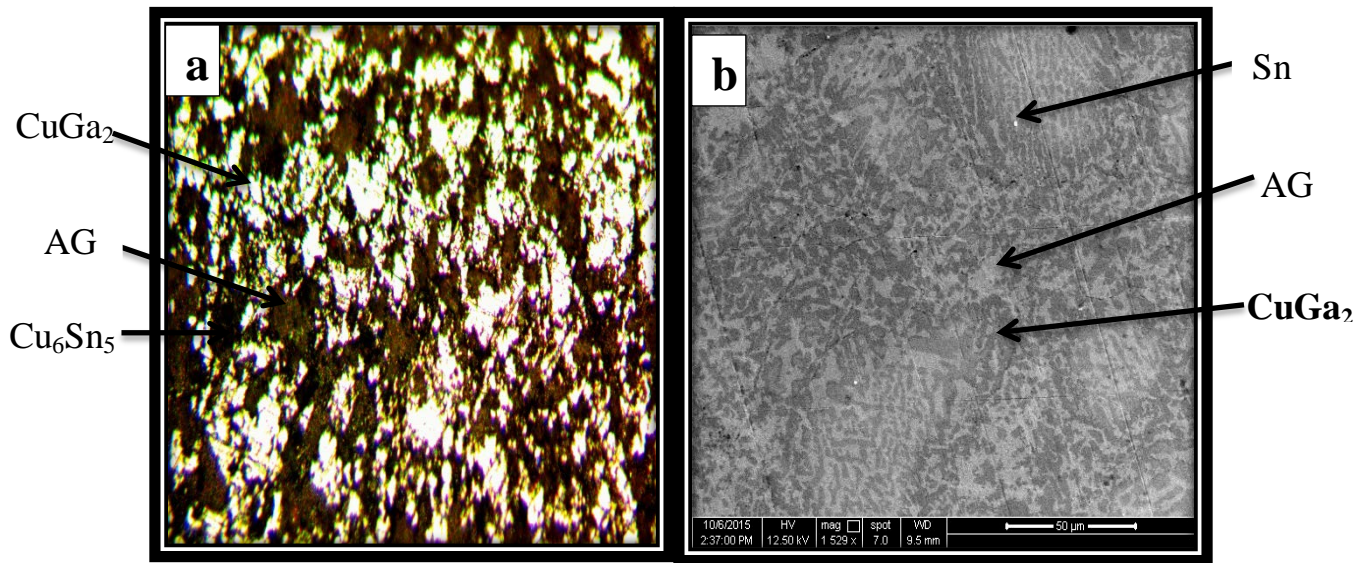


Figure (10) the microstructure observation of G1 alloy.  
a-By Optical Microscope at 400X magnification, b- By SEM.



Figure (11) The potentiodynamic polarization curve for M alloy.

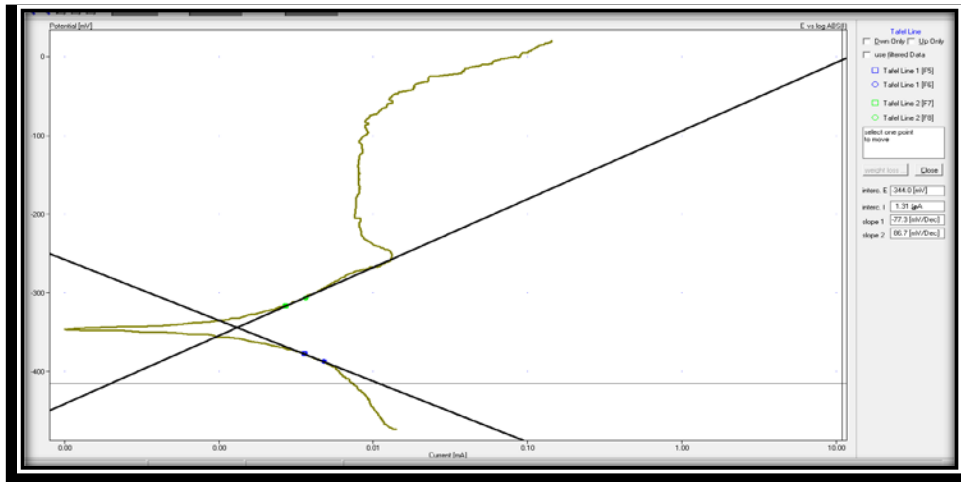


Figure (12) The potentiodynamic polarization curve for GI alloy.

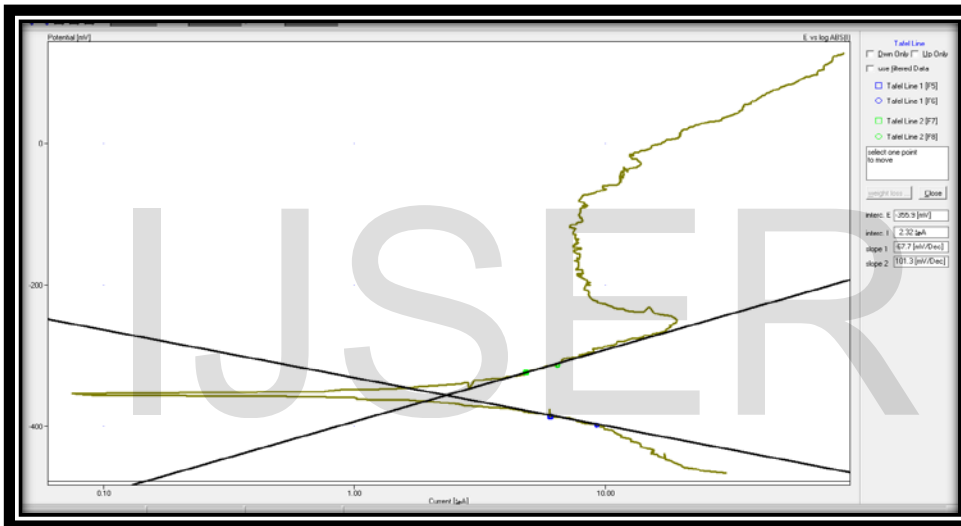


Figure (13) The potentiodynamic polarization curve for GS alloy.

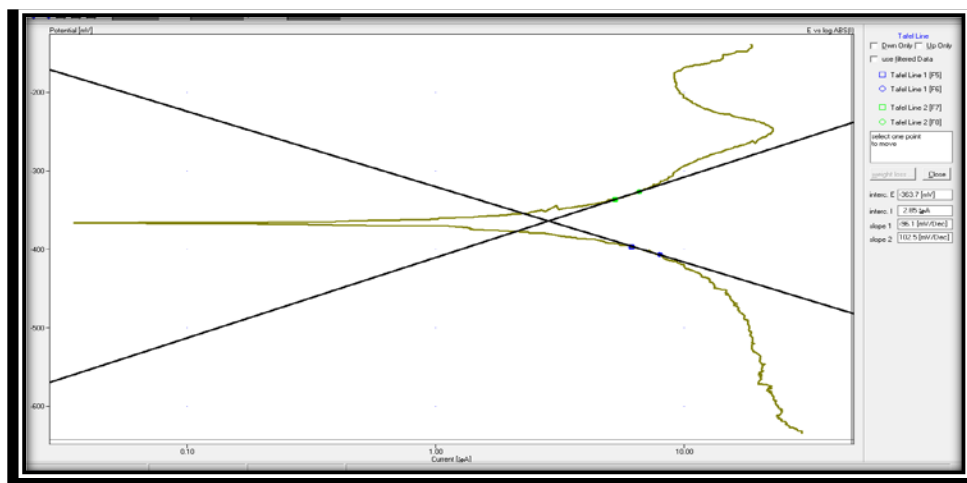


Figure (14) The potentiodynamic polarization curve for GIS alloy.

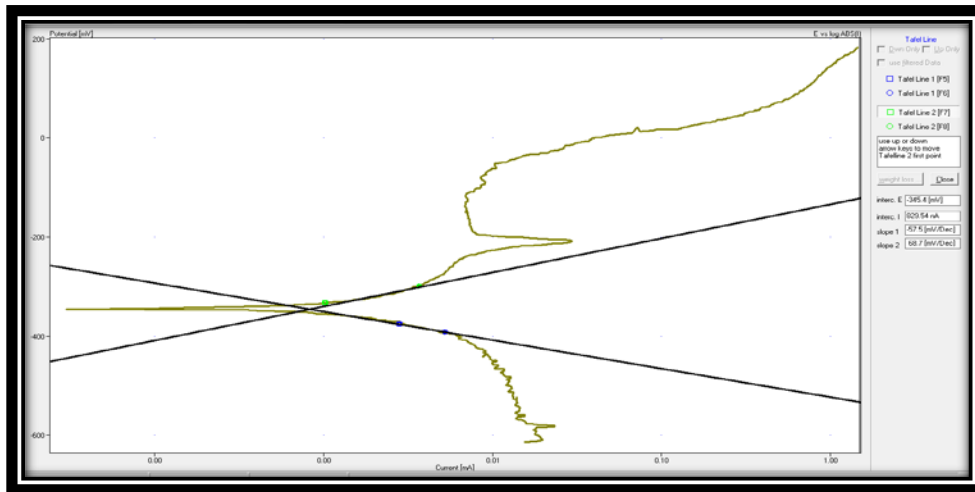


Figure (15) The potentiodynamic polarization curve for G1 alloy.

IJSER